

A new architecture for polymer transistors

Y. Yang & A. J. Heeger

UNIAX Corporation, 5375 Overpass Road, Santa Barbara, California 93111, USA

THE transistor, in its various forms, is a three-terminal amplifying electronic device¹. Transistors are usually based on inorganic semiconductors, such as silicon or gallium arsenide¹, but there is increasing interest in the use of organic semiconductors²⁻⁴, motivated by their structural flexibility and tunable electronic properties. The organic transistors fabricated to date have used a conventional 'field-effect' architecture; unfortunately, such devices involve relatively long conduction pathways which, owing to the low carrier mobilities of the organic materials, render them inherently slow. In an attempt to circumvent this problem, we have developed a different device geometry, more closely related to that of the vacuum-tube triode. The structure consists of a thin film of a semiconducting polymer sandwiched between two electrodes, with the third electrode—a layer of a porous metallic polymer⁵—embedded within the semiconductor. The third electrode plays a role similar to that of the grid in a vacuum tube, controlling the current flow between the two outermost electrodes. This thin-film architecture reduces the length of the conduction pathway, resulting in a relatively fast response time and, in contrast to conventional field-effect transistors, does not require lateral patterning.

The electronic structure of our device, the polymer grid triode (PGT), is analogous to that of an n-p-n (or a p-n-p) transistor¹ and similar to that of the permeable-base transistor⁶. The device can be viewed as constructed from two coupled diodes, connected back-to-back. Because polyaniline protonated with camphor sulphonic acid (PANI-CSA)⁷ has been used for the network grid electrode, we have focused on semiconducting polymer/electrode systems which are known to form high-quality tunnel diodes⁸; PANI-CSA/MEH-PPV/Ca and PANI-CSA/MEH-PPV/Al are important examples of such devices⁹ where MEH-PPV is the soluble derivative of poly(phenylene vinylene), poly(2-methoxy-5-(2'-ethyl-hexyloxy)-1,4-phenylene vinylene).

The electronic structure of the Al/MEH-PPV/PANI-network/MEH-PPV/Ca polymer grid triode is shown in Fig. 1. At zero bias (Fig. 1a), there is a common chemical potential. As a result of the different workfunctions of the Al, PANI-CSA and Ca, the built-in potential is analogous to that of an n-p-n transistor. Figure 1b shows the flat-band condition where current just begins to flow. At higher anode-to-cathode voltages (V_{AC}), the device is turned on. Figure 1c shows the case where electrons are injected into the π band of MEH-PPV at the Al electrode, and the electric field in the MEH-PPV forces the injected electrons towards the polymer grid. If the polymer network is of sufficiently low density, carriers will continue to still lower energy and be withdrawn at the Ca anode. Under these conditions, a current I_{AC} will flow in the external anode-to-cathode circuit. With reverse bias (negative voltage to the grid) on the input diode, I_{AC} is limited by the reversed bias current (Fig. 1d). If the rectification ratio is high, I_{AC} will be cut off by the bias voltage applied to the polymer grid. In Fig. 1, the Ca electrode is grounded (the anode), and the Al electrode is the cathode. These could be interchanged, with the Ca electrode used as the cathode and the Al electrode used as the anode.

The PGT structure with polymer grid electrode is sketched in Fig. 2, with the various constituents labelled. The first and second electrodes, (1) and (5), in either order, are the anode and cathode. The first (2), second (3'), and third (4) semiconducting polymers (all of which can be the same) serve to transport electronic charge carriers through the structure; the current due to

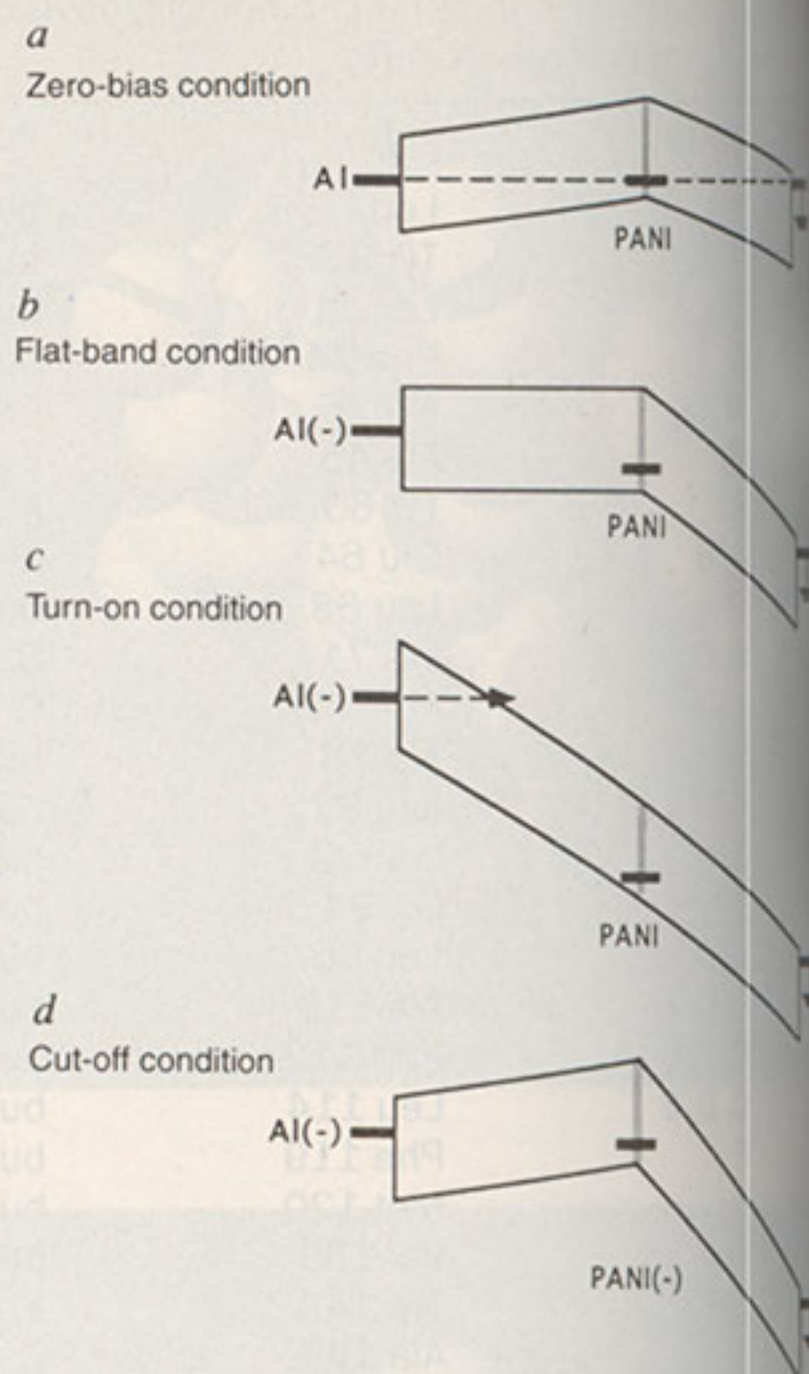


FIG. 1 Electronic structure of Al/MEH-PPV/PANI-network/MEH-PPV/Ca polymer grid triode: a, Zero-bias; b, flat-band condition; c, turn-on with electron transport from cathode to anode; d, cut-off with PANI-network/MEH-PPV/Al diode in reverse bias.

these charge carriers is controlled by the polymer grid (3). Symmetric PGTs can be made with (stable) Al as cathode and anode. Our initial work using Ca as one electrode in the PGT originates from the desire to characterize emission from the PANI-network/MEH-PPV/Ca diode. Light-emitting PGTs offer additional opportunities for three-terminal devices in which the emission can be switched on and off by V_G , with improved contrast relative to that from the simple diode¹⁰.

PANI-CSA self-assembles into a conducting network, blends with insulating host polymers^{5,11,12}. Near the percolation threshold, the network is fractal with high surface area and PANI-CSA/host interface. The connected pathways in the network cause such blends to exhibit electrical conductivities in excess of 1 S cm^{-1} at volume fractions of as low as a few per cent PANI-CSA. After selectively etching out the host polymer, the remaining conducting PANI-CSA network is porous, and has high surface area. The PANI-CSA network functions as a high-performance electrode for use in light-emitting diodes¹³. By filling the porous network with a semiconducting polymer, the contact area for carrier injection into the semiconducting polymer is increased. When the network is biased with respect to either the first or second electrode, the surface roughness, with pointed and sharp fibrillar features, enhances the local electric field in regions near the network. These same features are important when using the PANI-CSA network as the grid electrode in a PGT. Although any porous material which can be formed into a network could be used, the PANI-CSA network can be created spontaneously through self-assembly, a special advantage.

PANI-CSA solutions (2% w/w) were prepared using CH_2Cl_2 as the solvent⁷. A soluble polyester resin (PES) of low molecular mass ($M_r < 10,000$) was used for making blends with PANI-CSA; the PES was separately dissolved in CH_2Cl_2 at a concentration of 20% w/w. Blends of PANI-CSA/PES were prepared at concentrations of a few per cent (by mixing PANI-CSA and PES solutions at different ratios); above, but not

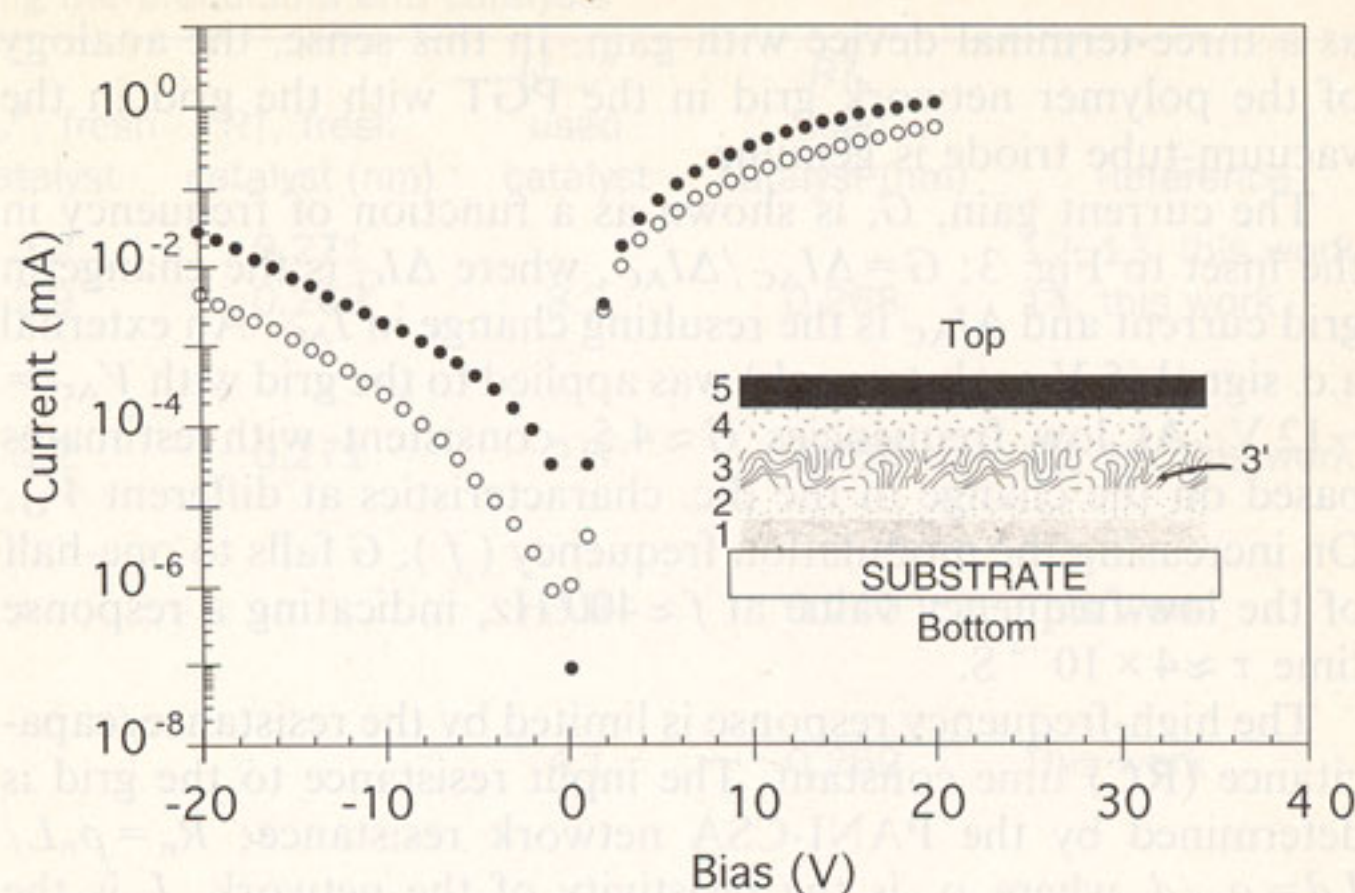
Main figure, plot of current versus voltage for the Al/MEH-PPV/ network half (open circles) and for the PANI-network/MEH-PPV/ (filled circles) of the PGT; both exhibit diode behaviour. Inset, structure of the PGT: (1), first electrode; (2), semiconducting (3), PANI-CSA grid electrode filled with (3') semiconducting (4), semiconducting polymer and (5), second electrode.

the percolation threshold^{11,12}. At high concentrations, the network does not allow carriers to pass through the very low concentrations, the 'network' breaks up into disconnected regions¹².

To fabricate the PGT, the Al anode was first vacuum-deposited onto a glass substrate. The first MEH-PPV layer (10 Å) was then spin-cast from solution in xylene⁵. To make a polymer grid, a PANI-CSA blend (3% w/w) layer was spin-cast onto the first MEH-PPV layer and dried in air at 50 °C for 24 h. MEH-PPV was then spin-cast from xylene directly onto the PANI:PES blend thin film. As xylene is an excellent solvent for PES, the PES in the PANI:PES blend was etched into the xylene and subsequently carried away by the solvent during the spin-casting process¹³. Hence in a single step, MEH-PPV replaced PES to fill (or partially fill) the voids in the porous network within the PANI network. Typical film thicknesses for the PANI network electrode filled with semiconducting material range from 100 to 700 Å. The MEH-PPV layer extended beyond the PANI network to form the third semiconducting layer, shown as layer 3' in Fig. 2. After vapour deposition of the thin Ca film (at 0.1 Å) on top, the PGT has continuous semiconducting polymer between the anode and cathode, with the PANI-CSA grid network embedded within the polymer semiconductor. More than 20 devices have been made, with excellent reproducibility.

Figure 2 shows typical measurements of I versus V for the Al/MEH-PPV/PANI-network half of the device and for the PANI-network/MEH-PPV/Ca half of the device show that both exhibit diode behaviour with modest rectification ratios. The data are shown in Fig. 2.

Figure 3 shows the plot of I_{AC} versus V_{AC} for an Al/MEH-PPV/PANI-network/MEH-PPV/Ca polymer grid triode is shown in Fig. 3 for



various grid voltages, V_G , applied between the network grid and the cathode. In this single carrier ('electron-only') PGT, electrons are injected at the Al cathode and withdrawn at the Ca anode (or *vice versa*). As the PANI grid is made negative with respect to the Al and Ca electrodes, I_{AC} is suppressed. Generally, with $V_G = -V_0$, $I_{AC} \approx 0$ until $V_{AC} > V_0$.

When $V_G > 0$, the injected electrons are withdrawn at the positive PANI-CSA grid. In addition, when the PANI-network/MEH-PPV/Ca diode is under forward bias, holes are injected at the PANI-CSA/MEH-PPV interface. As expected for positive V_G , the PANI-network/MEH-PPV/Ca diode emits light. This emission has been characterized in detail¹⁰.

The electronic structure diagrams of Fig. 1 imply that I_{AC} will begin to flow when the PANI-network/MEH-PPV/Al diode is in the flat-band condition. Figure 3 shows that for successively higher $|V_G|$, the steep onset of I_{AC} (which defines the flat-band condition) moves to higher values of $|V_{AC}|$. Qualitatively, the I_{AC} versus V_{AC} characteristics shown in Fig. 3 are consistent with the electronic structure diagrams of Fig. 1. For $V_G < 0$, electrons injected at the Al cathode pass through the PANI-CSA grid when $|V_{AC}| > |V_G|$. Thus the PANI-CSA network is sufficiently open to allow electron current to flow and to function as a control grid.

As PANI-CSA is an excellent 'hole injector' for MEH-PPV⁹, PANI-CSA is also an excellent 'electron extractor' from MEH-PPV. Thus when the PANI-CSA 'grid' electrode was replaced with a continuous PANI-CSA film, all the current passed through the grid circuit. With a solid metal film between the two MEH-PPV layers, the device is simply two diodes connected back-to-back; the two diodes are not coupled to form a PGT. Such a two-diode device can function as a current switch, but not

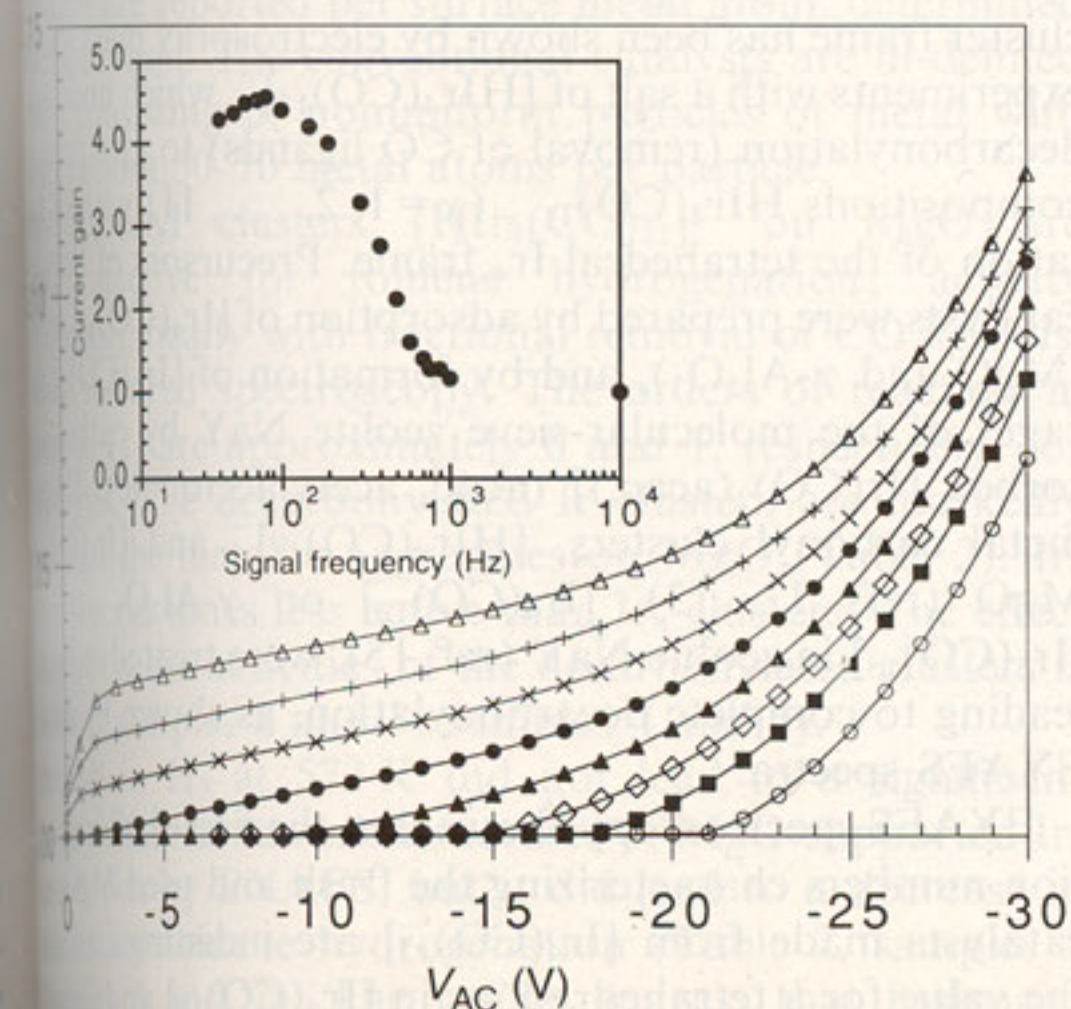


FIG. 3 Main figure, plot of anode-to-cathode current I_{AC} versus anode-to-cathode voltage (V_{AC}) for various grid voltages, V_G , between the PANI-CSA network grid and the cathode: Δ , $V_G = 3.1$ V; +, $V_G = 2.61$ V; \times , $V_G = 2.1$ V; \bullet , $V_G = 0$ V; \blacktriangle , $V_G = -8$ V; \diamond , $V_G = -13.3$ V; \blacklozenge , $V_G = -16.4$ V; \circ , $V_G = -20$ V. Inset, current gain as a function of frequency.

as a three-terminal device with gain. In this sense, the analogy of the polymer network grid in the PGT with the grid in the vacuum-tube triode is genuine.

The current gain, G , is shown as a function of frequency in the inset to Fig. 3; $G = \Delta I_{AC} / \Delta I_{DC}$, where ΔI_G is the change in grid current and ΔI_{AC} is the resulting change in I_{AC} . An external a.c. signal (5 V peak-to-peak) was applied to the grid with $V_{AC} = -12$ V. At low frequencies $G \approx 4.5$, consistent with estimates based on the change in the d.c. characteristics at different V_G . On increasing the modulation frequency (f), G falls to one-half of the low-frequency value at $f \approx 400$ Hz, indicating a response time $\tau \approx 4 \times 10^{-4}$ s.

The high-frequency response is limited by the resistance/capacitance (RC) time constant. The input resistance to the grid is determined by the PANI-CSA network resistance; $R_n = \rho_n L / Ld = \rho_n / d$, where ρ_n is the resistivity of the network, L is the lateral dimension (assuming a square device) and d is the thickness of the device. The capacitance is determined by the thin-film ('capacitor') geometry, $C = \epsilon_s A / d = \epsilon_s L^2 / d$, where ϵ_s is the dielectric constant of the semiconductor. Thus $\tau_{RC} = RC =$

$\rho_n \epsilon_s (L/d)^2$. The measured values of R_n and C are consistent with the high-frequency cut-off shown in Fig. 3. The device area in this initial study was 0.2×0.6 cm. Size reduction would increase the RC-limited frequency response; by decreasing the lateral dimensions to 100 μm , $1/\tau_{RC} \approx 10^6 \text{ s}^{-1}$.

The theoretical limit for the high-frequency cut-off can be estimated. To obtain significant gain, carriers must move through the grid in a time comparable with the period of the a.c. signal. The carrier velocity is $2\mu V_G / d$, where μ is the carrier mobility. Thus, the μ -limited response time is $\tau_i \approx d^2 / 2\mu V_G$. With $V_G = 5$ V and $d = 2,500$ Å, $\tau_i \approx 4 \times 10^{-3} \mu$. For example, with $\mu \approx 10^{-4} \text{ cm}^2 \text{ V}^{-1} \text{ s}^{-1}$, as reported for semiconducting polymers^{2,3}, $\tau_i \approx 4 \times 10^{-7}$ s. The short response time with such a small mobility is a direct result of the thin-film architecture of the polymer grid triode.

Higher gain can be achieved by improving the rectification ratios of the back-to-back diodes, by making the overall structure (and the component layers) thinner, by optimizing the concentration of PANI-CSA in the network for optimum transmission of carriers through the network grid, and by using a polymer semiconductor with a higher mobility. □

Received 12 August; accepted 21 October 1994.

1. Sze, S. M. *Physics of Semiconductor Devices* (Wiley, New York, 1981).
2. Burroughs, J. H., Jones, C. A. & Friend, R. H. *Nature* **325**, 137–141 (1988).
3. Assadi, A. et al. *Synth. Met.* **37**, 123–130 (1990).
4. Garnier, F. et al. *Science* **265**, 1684–1686 (1994).
5. Yang, C. Y., Cao, Y., Smith, P. & Heeger, A. J. *Synth. Met.* **53**, 293–301 (1993).

6. Bozler, C. O. et al. *Surf. Sci.* **74**, 487–500 (1986).
7. Cao, Y., Smith, P. & Heeger, A. J. *Synth. Met.* **48**, 91–97 (1992).
8. Parker, I. D. J. *Appl. Phys.* **75**, 1656–1666 (1994).
9. Yang, Y. & Heeger, A. J. *Appl. Phys. Lett.* **64**, 1245–1247 (1994).
10. Yang, Y. & Heeger, A. J. *US Patent Applic.* No. 08/227 979.
11. Reghu, M. et al. *Macromolecules* **26**, 7245–7249 (1994).
12. Reghu, M. et al. *Phys. Rev. B* (in the press).
13. Yang, Y. et al. *J. appl. Phys.* (in the press).

Size-dependent catalytic activity of supported metal clusters

Z. Xu*, F.-S. Xiao*†, S. K. Purnell*‡, O. Alexeev*, S. Kawi*§, S. E. Deutsch* & B. C. Gates*||

* Department of Chemical Engineering and Materials Science, University of California, Davis, California 95616, USA

BECAUSE catalysis by metals is a surface phenomenon, many technological catalysts contain small (typically nanometre-sized) supported metal particles with a large fraction of the atoms exposed¹. Many reactions, such as hydrocarbon hydrogenations, are structure-insensitive, proceeding at approximately the same rate on metal particles of various sizes provided that they are larger than about 1 nm and show bulk-like metallic behaviour¹. But it is not known whether the catalytic properties of metal particles become size-dependent as the particles become so small that they are no longer metallic in character. Here we investigate the catalytic behaviour of precisely defined clusters of just four and six iridium atoms on solid supports. We find that the Ir₄ and Ir₆ clusters differ in catalytic activity both from each other and from metallic Ir particles. This raises the possibility of tailoring the catalytic behaviour of metal clusters by controlling the cluster size.

Investigations of gas-metal clusters demonstrate that their reactivities depend strongly on their structures. Reactions of D₂ with Fe, Ni, Pd and Pt clusters show striking patterns of both reaction rates and coverage of clusters with D ligands depending on the metal, and the charge and number of atoms in the cluster^{2,3}. The reactivity of gas-phase Co₄⁺ for dehydrogenation of cyclohexane to give benzene⁴ is markedly different from that

of Co clusters with only one atom more or one atom less, and the reactivity of Fe₄⁺ for formation of benzene from smaller hydrocarbons is similarly unique⁵.

The fascination with molecular metal clusters⁶ motivated many investigations of their catalytic properties, but few examples of molecular cluster catalysis and no industrial applications have emerged^{7,8}. A decisive limitation is the lack of stability of most ligand-stabilized clusters. But metal clusters dispersed on solid supports have been thought to exist among the complex mixtures of structures in industrial supported metal catalysts; recently, clusters of (on average) 5–6 Pt atoms in the pores of zeolite LTL have been identified by extended X-ray absorption fine structure (EXAFS) spectroscopy⁹ and applied industrially as catalysts for selective reforming of naphtha to give aromatics^{10,11}. Thus the metal clusters of most importance as catalysts are robust supported clusters and not molecular clusters.

We have investigated the catalytic activities of Ir₄ and Ir₆ clusters on porous metal oxide supports for structure-insensitive hydrocarbon hydrogenation reactions. The robustness of the Ir₄ cluster frame has been shown by electrospray mass spectrometry experiments with a salt of [HIr₄(CO)₁₁][−], which underwent clean decarbonylation (removal of CO ligands) to give products with compositions HIr₄(CO)_{11−x} ($x = 1, 2, \dots, 11$) without fragmentation of the tetrahedral Ir₄ frame. Precursors of the supported catalysts were prepared by adsorption of [Ir₄(CO)₁₂] on supports (MgO and γ -Al₂O₃), and by formation of [Ir₆(CO)₁₆] in supercages of the molecular-sieve zeolite NaY by carbonylation of sorbed [Ir(CO)₂(acac)] (acac, acetylacetonate). The resultant metal carbonyl clusters, [HIr₄(CO)₁₁][−] and [Ir₆(CO)₁₅]^{2−} on MgO (refs 12, 13), [Ir₄(CO)₁₂] on γ -Al₂O₃ (ref. 14) and [Ir₆(CO)₁₅] in zeolite NaY (ref. 15), were treated in He at 573 K, leading to complete decarbonylation, as shown by infrared and EXAFS spectra.

EXAFS spectroscopy shows that the first-shell Ir–Ir coordination numbers characterizing the fresh and used MgO-supported catalysts made from [Ir₄(CO)₁₂] are indistinguishable from 3, the value for a tetrahedron, as in [Ir₄(CO)₁₂] and [HIr₄(CO)₁₁][−]

Present addresses: † Department of Chemistry, Jilin University, Changchun 130023, People's Republic of China; ‡ W. R. Grace and Co., 5603 Chemical Road, Baltimore, Maryland 21226, USA; § Department of Chemical Engineering, National University of Singapore, Singapore 0511. || To whom correspondence should be addressed.